

CONSTRUCTION OF A 12 GHz TOTAL POWER RADIO TELESCOPE FOR TEACHING PURPOSES, SUITABLE FOR NOISY ENVIRONMENTS, USING SATELLITE TV DEVICES

Maurizio Tinti*

D.E.I.S., Università di Bologna, Bologna, Italy

Abstract—Schools and universities often need to support theoretical lectures on Radio Astronomy with practical lessons; in addition, science centres need instruments to explain this subject to the general public. However, professional radio telescopes are largely inaccessible to students and the public, because they tend to be very costly and are still fairly uncommon. It would seem, therefore, interesting to explore the possibility of designing a low-cost radio telescope for teaching purposes. The most critical part of a radio telescope is its receiver; considering the low intensity of radiation from the radio sky, this needs, among other features, to be very sensitive, necessitating the use of expensive low noise amplifiers, often cooled to low temperatures. For some time now, low-cost components for the reception of satellite TV have been available on the consumer market. These are known as Low Noise Block (LNB) and they include, as a front-end, an amplifier with very low intrinsic noise. In this study, we wanted to test the feasibility of designing and using a 12 GHz total power demonstrative radio telescope, using, as a front-end, an LNB mounted in the focus of an offset parabolic mirror. Unlike other designs, we made the system suitable for environments with high electromagnetic noise, such as schools in urban centres, by using a bandpass filter in the Intermediate Frequency section.

1. INTRODUCTION

Figure 1 shows the block diagram of a “total power” radio telescope.

The noise power coming from the radio source under observation is firstly amplified by a Radio Frequency (RF) amplifier. The next block

Received 31 May 2012, Accepted 6 February 2013, Scheduled 7 February 2013

* Corresponding author: Maurizio Tinti (maurizio.tinti@unibo.it).

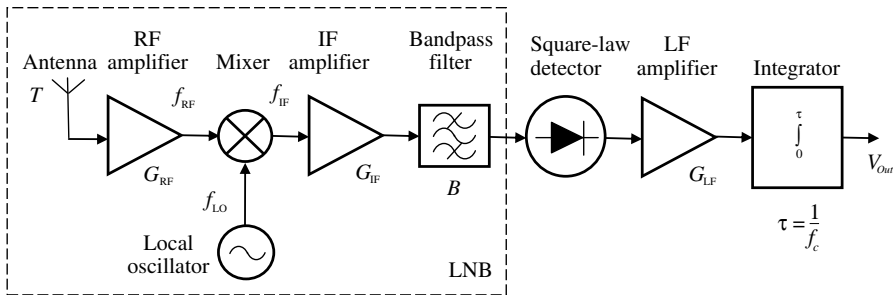


Figure 1. Block diagram of a “total power” radio telescope. We have indicated with: T the temperature of the antenna, G_{RF} the gain of the Radio Frequency (RF) amplifier, f_{RF} the frequency of the RF signal, f_{LO} the frequency of the local oscillator, f_{IF} the frequency of the Intermediate Frequency (IF) signal, G_{IF} the gain of the IF amplifier, B the bandwidth of the bandpass filter, G_{LF} the gain of the Low Frequency (LF) amplifier, τ the time constant of the integrator.

is a mixer that converts the RF signal to the Intermediate Frequency (IF) signal, which is amplified by the IF amplifier and band limited by a bandpass filter. The IF signal, like the RF signal, is comparable to a randomly modulated carrier wave. Its power is then measured by a square law detector. This is followed by a Low Frequency (LF) amplifier and by an integrator, whose time constant τ determines the minimum detectable temperature of the system [1]. This time constant is set so as to achieve a compromise between the conflicting demands of having a sufficiently short response time compared to the dynamics of the phenomena that the system observes and high receiver sensitivity.

Another factor which determines the minimum detectable temperature of the system is the noise figure of the front-end amplifier [1], which should be very low. In professional radio telescopes, expensive low-noise amplifiers are used to achieve this. In our project, we tested the possibility of using, as a front-end receiver, an LNB, which includes a very low noise amplifier.

2. CALCULATIONS REGARDING THE OBSERVING SYSTEM

The equivalent noise temperature T_R of the receiver is determined by that of the front-end amplifier. The front-end amplifier of the LNB that we used has, as indicated by the manufacturer, a noise figure

$NF = 0.3$ dB. Assuming the ambient temperature $T_0 = 290$ K, is [1]:

$$T_R = T_0 \left(10^{\frac{NF}{10}} - 1 \right) = 20.7 \text{ K.} \quad (1)$$

Assuming the temperature of the Cold Sky $T_{\text{Cold Sky}} \approx 40$ K, the temperature of the system is [1]:

$$T_{sys} = T_R + T_{\text{Cold Sky}} \approx 60 \text{ K} \quad (2)$$

Therefore, the minimum detectable temperature of the system is, having fixed the bandwidth $\Delta\nu$ of the bandpass filter that we inserted in the IF section = 200 MHz and the time constant τ of the integrator = 10 s [1, 4]:

$$\Delta T_{\min} = \frac{T_{Sys}}{\sqrt{\Delta\nu \cdot \tau}} = \frac{60}{\sqrt{200 \cdot 10^6 \cdot 10}} = 1.3 \cdot 10^{-3} \text{ K} \quad (3)$$

The manufacturer indicates the efficiency of the parabolic mirror as being equal to 60%, an attenuation of the posterior lobes with respect to the main lobe of 45 dB (or $10^{\frac{45}{10}} \cong 31622$) and an aperture beam angle at -3 dB of 3° .

If we point the antenna towards the strongest radio source, which is the Sun ($T \approx 6000$ K), taking into account that the angle subtended by the Sun if seen from Earth is 0.5° , and thus in this case the fraction of the antenna's area that is invested by the Sun radiation is $\frac{0.5}{3} \cong 0.16$, then the temperature that we can measure is 1000 K. This effect is called "dilution effect". The difference between the measured Sun temperature and the Cold Sky temperature is much smaller than the minimum detectable temperature of the system; we can therefore say that with a radio telescope designed using an LNB we can at least detect the Sun.

The noise power received when the antenna is pointing towards the Cold Sky also taking into account the fact that the posterior lobes point to the ground ($T \approx 300$ K) [1], is, having indicated with $k = 1.38 \cdot 10^{-23} \text{ JK}^{-1}$ the Boltzmann's constant:

$$\begin{aligned} W_{\text{Cold Sky}} &= k \cdot \left(0.6 \cdot T_{\text{Cold Sky}} + \frac{0.6}{31622} T_{\text{Earth}} + T_R \right) \cdot \Delta\nu \\ &\cong 0.12 \cdot 10^{-12} \text{ W} \approx -99.1 \text{ dBm.} \end{aligned} \quad (4)$$

When the antenna points towards the Sun, the received power is:

$$\begin{aligned} W_{\text{Sun}} &= k \cdot \left(0.6 \cdot T_{\text{Cold Sky}} + \frac{0.6}{31622} T_{\text{Earth}} + 0.6 \frac{0.5}{3} T_{\text{Sun}} + T_R \right) \cdot \Delta\nu \\ &\cong 1.78 \cdot 10^{-12} \text{ W} \approx -87.5 \text{ dBm} \end{aligned} \quad (5)$$

The radiometer input signals thus have a dynamic of 11.6 dB.

3. DESCRIPTION OF THE SYSTEM

An LNB amplifies the input signal in the frequency range between 11 GHz and 12 GHz and converts it to the IF (1 to 2 GHz). The overall gain of the block is about 60 dB over a bandwidth of about 1 GHz.

Since the nature of the proposed radio telescope is purely for teaching purposes, it is possible to accept a merely qualitative indication [2, 3]. In order to keep to a low level the gain of the DC section that follows the detector (which introduces noise and thermal drift), it is possible to increase the gain of the IF section by inserting an amplifier between the LNB and the detector. We can use, for example, a linear amplifier for satellite TV (20 dB gain) together with another commercially available amplifier, such as the Mini-Circuits ZEL-1217LN (20 dB gain).

The presence of interference from man made radio signals may require the bandwidth of the receive to be limited. After considerable experimentation (we made many observations of the Sun and the Moon in three different sites which are significative for environmental noise: in the city centre of Bologna, in the suburbs of the city on the terrace of the Institute of Radio Astronomy and in the country near the house of Guglielmo Marconi in Pontecchio) it became clear that it was necessary to limit the bandwidth to a $\Delta\nu = 200$ MHz. Despite so much band reduction, the equipment still demonstrates a good degree of functionality relative to its geographical positioning, i.e., large urban or rural sites. This bandwidth limitation can be obtained by inserting a filter between the two amplifiers, taking into account their potentially different load impedances.

As our receiver is intended for observing sources of non-polarized fields, the LNB can be supplied with 12 or 18 DC volts, which would normally select the polarization of the accepted input signal.

The DC section consists of an integrator circuit and an offset circuit. The proposed value for the integrator time constant τ was determined experimentally as 10 s, considering the observational dynamics of the equipment. With this value of τ we can observe a Sun transit without distortion.

The offset circuit, placed after the integrator, consists of an adder circuit and through a manual adjustment, allows a DC level to be subtracted from the detected signal. When the system is only receiving the electromagnetic background (antenna pointing towards the Cold Sky), it is possible to subtract a voltage equal to the corresponding level of the detector output, reducing to zero the indication on the measuring instrument, thus carrying out an “offset” operation. In this way, the radio telescope will measure only the difference between the

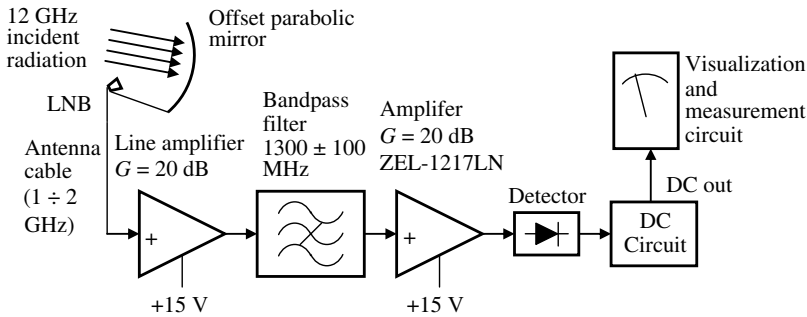


Figure 2. Block diagram of the receiving system.

electromagnetic background and the radiation emitted by the source towards which the antenna is aimed.

In addition to the measuring instrument (consisting of a voltmeter), the output signal can also be sent to a device that displays the time trend, such as an oscilloscope, or to a data acquisition card connected to a computer.

The block diagram of the system is shown in Figure 2.

4. DESIGN AND IMPLEMENTATION OF THE BANDPASS FILTER

The bandpass filter that was built is of the mechanically modified combline type. It is shown in Figure 3.

This solution has the following advantages:

- the mutual coupling between the resonators required by the bandwidth expected is easily obtained in a small space and the implementation is thus more compact;
- the tolerances required for the implementation of these filters are relatively high;
- the losses are extremely low;
- the interdigitated filters are easy to design, build and tune and the selectivity that can be achieved is appropriate for our application.

The filter was designed using Dishal's method [8,9]. The tuned circuits are made up of rectangular resonators, with a thickness of 0.4 mm, width 0.8 mm and length about $\lambda_c/4$ (λ_c is the wavelength corresponding to the center frequency f_c of the signal applied to the filter) mounted alternately on opposite sides of the container (the container being a Teko standard model 371.16 external dimensions

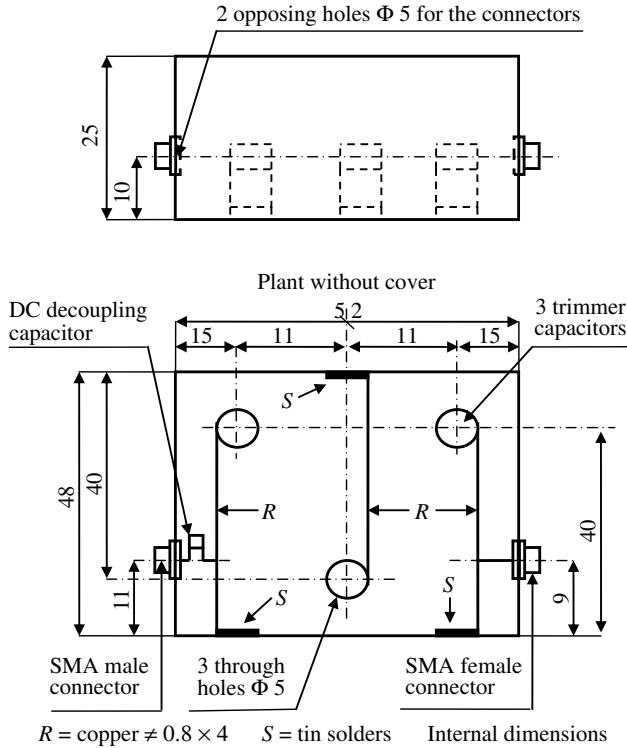


Figure 3. Drawing of the bandpass filter.

$54 \times 50 \times 26$, galvanized sheet $\neq 1$). To make it possible to tune the filter, three trimmer capacitors for SHF (value 1.5–10 pF) were connected between the ends of the resonators and the side wall of the container.

Measurements of the filter bandwidth and return loss are shown in Figure 4, its implementation is shown in Figure 8. The Q factor of each resonator is hardly measurable. We have measured the Q factor of the whole filter, which is about 7, according with the definition equal to the ratio between the filter's resonance frequency and its bandwidth.

5. DESIGN OF THE DETECTOR CIRCUIT

In this study we designed a specific detector for the application.

To maximize the detector output signal we needed to provide an impedance matching between the last amplifier of the amplification chain and the detector. In our situation, with large signals, the diode

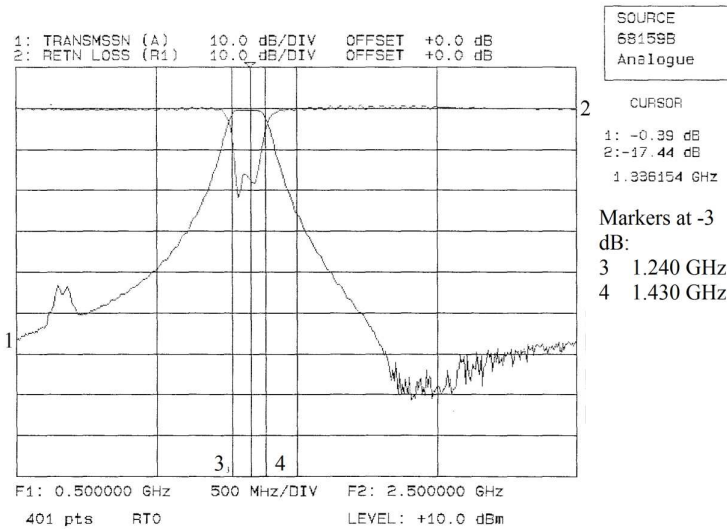


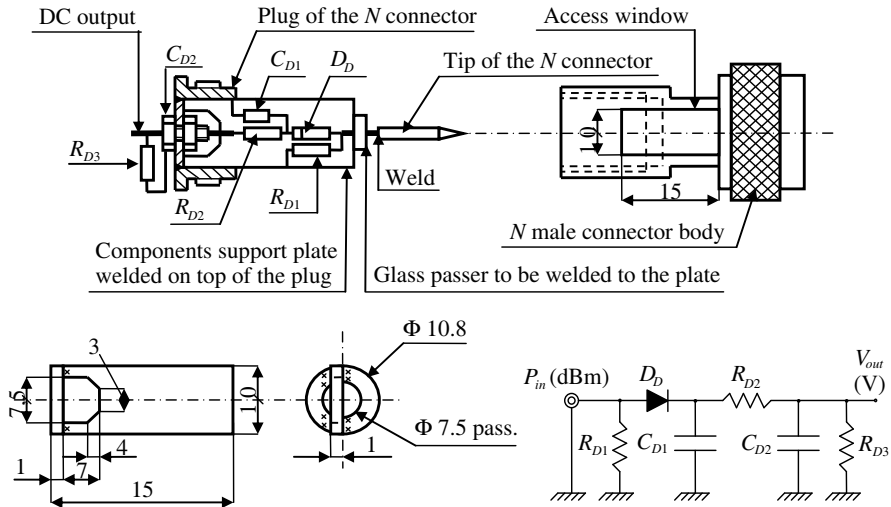
Figure 4. Measurements of the IF filter using a vector network analyzer HP 8722 D. The measures displayed confirm clearly the predictions made in the theoretical calculation. The insertion loss of only 0.39 dB and the return loss, which is on average 20 dB in the band of operation, reflect a very good performance.

is alternately in conduction and in interdiction, and consequently is a time variant load that could cause malfunctions in the last amplifier of the amplification chain and in the preceding stages. It was thus decided, in the design of the detector circuit, to adopt a simplified approach of adaptation and isolation, for which the topology of the detector circuit turned out to be as shown in Figure 5. As shown in the figure, the detector circuit has been housed within an N connector.

The purposes of the resistor $R_{D1} = 56 \Omega$ at the input of the detector circuit are as follows:

- to contribute to the impedance adaptation between the detector input and the output impedance of the preceding stage (which is 50Ω);
- to close the input of the diode detector for the DC component, if this is not done at the output of the preceding stage.

The detected voltage is taken via R_{D2} , which helps to reduce the excursion of the input impedance of the detector circuit (with consequent widening of the band); however, its presence means a decrease in the detector sensitivity. In fact, the DC voltage taken from the voltage divider formed by R_{D2} and R_{D3} depends on the values



Components support plate. Material: Brass \neq 1. Tin solders.

Figure 5. Detector's drawing and circuit.

of these resistors; a compromise value for R_{D2} that does not reduce too much the detection efficiency can be: $R_{D2} = \frac{1}{10}R_{D3}$. Because the value of R_{D3} is set at $10\text{ k}\Omega$ (so the detector is not loaded by the following circuit, which has an input impedance of $1\text{ M}\Omega$) the value of R_{D2} will be $1\text{ k}\Omega$. It was observed that with these values of R_{D2} and R_{D3} the impedance in parallel to R_{D1} is much higher than R_{D1} , both when the diode is interdicted and when it is in conduction, so the input impedance of the detector circuit is about $50\ \Omega$, as required by the preceding amplifier.

C_{D1} e C_{D2} were calculated in order to have the maximum detection efficiency, given the conditions of non-distortion of the signal to be detected [5–7].

For C_{D1} we used a ceramic capacitor, value 470 pF ; for C_{D2} , because it is placed at the output of the container, we used a passing capacitor, value 1 nF .

The detection characteristic was then measured and compared with that of the commercial detector HP 423A, as shown in Figure 6. The implementation of the detector is shown in Figure 8.

6. DC CIRCUIT

From Figure 6 we can see, taking into account the gain of the IF section, that corresponding to the minimum input power ($1.2\text{ mW} = 0.79\text{ dBm}$) there is a detector output voltage of about 120 mV and corresponding

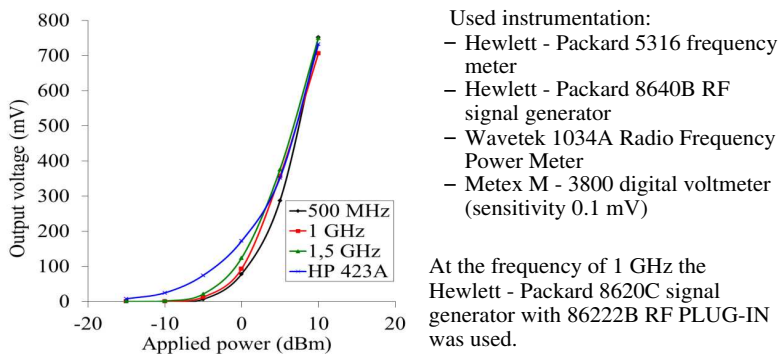


Figure 6. Measures on the detector circuit in semi-logarithmic scale. The commercial detector HP423@1.5 GHz was measured at only one frequency (1.5 GHz).

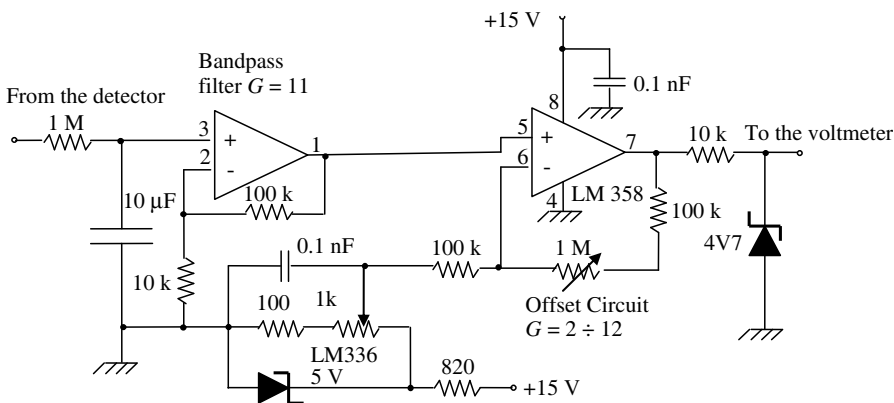


Figure 7. DC circuit.

to the maximum input power (17.8 mW = 12.5 dBm) a detector output voltage of about 700 mV. To bring the output signal to a dynamic compliant with that of a data acquisition circuit (0–5 V), the gain of the DC circuit will be approximately 10. In fact, because of the losses in the antenna cable and the components connections of the amplification chain, the DC gain of the circuit can have the capability to be adjusted up to 100. The schematic of the DC circuit is shown in Figure 7.

The implementation of the DC Circuit is shown in Figure 8.

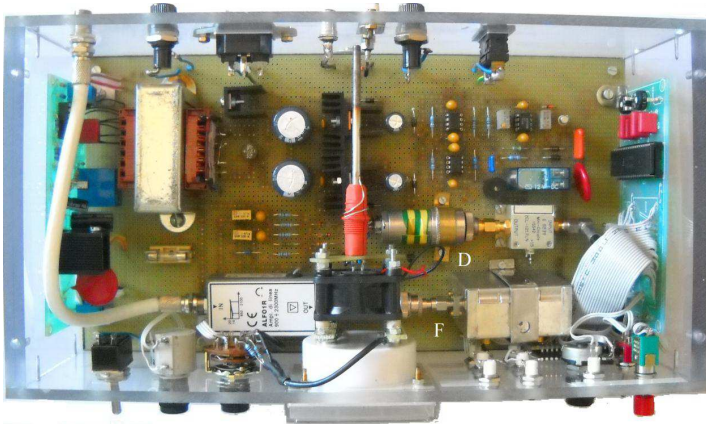


Figure 8. Implementation of the radio telescope. F: bandpass filter; D: detector.

7. PRACTICAL USE OF THE RADIO TELESCOPE

In spring 2012 the developed instrument was tested in Bologna on the terrace of the Institute of Radio Astronomy of the National Institute of Astrophysics, making observations of the Sun, the Moon and the Galaxy. Figure 9 shows the expected graphical standard response of any strong radio source like the Sun, the Moon or the Galaxy while slowly horizontally crossed by the antenna main beam. Numerical values are not indicated on the axis because the observations can be only qualitative, according to the use of the radio telescope. The teacher or the experienced observer, after this experimental initial test may calibrate the instrument by setting gain, time of crossing of the source and registration devices in order to get a repeatable performance.

In Figure 10 it is shown the system in operation in the centre of Bologna.

8. DISCUSSION

This receiver is not required to have the specifications to accurately measure the temperature of hot bodies identified by the beam of its parabolic antenna. A receiver for such a task would take the more prestigious aspect of a radiometer designed according to the criteria of high stability ($10^{-3} \dots 10^{-4} \text{ grad.}^{-1}$) of the gain of the amplifier stages, or even that of the sophisticated “Dicke receiver”, only necessary in radio astronomy research at the highest level. The design

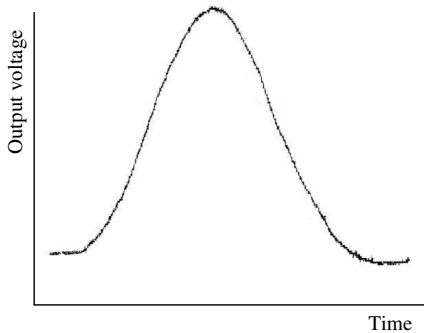


Figure 9. A slow crossing of a strong radio source through the antenna main beam. The figure shows the Moon at 86° azimuth and 19.7° elevation.



Figure 10. The radio telescope in operation.

specifications of this receiver, however, did not provide for accurate numerical determination of the temperatures involved. Ensuring a sufficient S/N ratio, by choosing appropriate electronic devices, we were concerned about the gain of the amplifier chain, estimated to be over 100 dB, needed to achieve the required output levels. It is easy to see that, in presence of such gains, even small variations in the physical temperature of the electronic components can easily, even in our application, introduce unacceptable variations, i.e., of some critical voltages such as that of the post detection DC level. As a result of careful measurements and also considering the limits of variability of the temperature when in position, it was decided that the entire receiver should be thermostated at a temperature of approximately 40°C .

After the implementation of these initial conditions the issue of verification of the radio-electric performance was considered. The actual temperatures involved at the receiver input unfortunately tend to significantly deteriorate the S/N ratio computable from the above data. It is necessary to consider the secondary lobes of the antenna which sense, although in a reduced manner, the temperature of all surrounding objects, the noise temperature of the front end of the receiver, the low efficiency of the antenna and its “dilution effect” that occurs when the surface of the hot body to be measured is smaller than

the area of the primary beam of the antenna.

Considering all the factors mentioned above, an estimation of the input temperatures of the receiving system enables us to evaluate the working S/N ratio, which is low but still higher than the theoretical limit, in order to ensure a proper functioning of the equipment under discussion.

ACKNOWLEDGMENT

I would like to thank Dr. Goliardo Tomassetti from I.R.A-I.N.A.F. Bologna, Professor Gabriele Falciasecca and Margaret Baigent from the Università di Bologna for their kind cooperation.

REFERENCES

1. Kraus, J. D., *Radio Astronomy*, McGraw-Hill Book Company, New York, 1966.
2. Bell, D. A., *Electrical Noise*, D. Van Nostrand Company, Inc., Princeton, NJ, 1960.
3. Kac, M. and A. J. F. Siegert, "On the theory of noise in radio receivers with square law detectors," *J. Appl. Phys.*, Vol. 18, 383, 1947.
4. Tiuri, M. E., "Radio astronomy receivers," *IEEE Trans. Antennas, Propagation*, Vol. 12, 930–938, December 1964.
5. De Castro, E., *Fondamenti di Comunicazioni Elettriche*, Zanichelli, Bologna, 1967.
6. Dammers, B. G., J. Haantjes, J. Otte, and H. van Suchtelen, *Application of the Electronic Valve in Radio Receivers and Amplifiers*, book IV, N. V. Philips' Gloeilampenfabrieken, Technical and Scientific Literature Department, Eindhoven, Netherlands, 1950.
7. Seely, S., *Radio Electronics*, McGraw-Hill Book Company, New York, 1956.
8. White, I., "A simple way to design narrowband interdigital filters," *Radio Communication*, February 1984.
9. Dishal, M., "A simple design procedure for small percentage bandwidth round-rod interdigital filters," *IEEE Transactions on Microwave Theory and Techniques*, Vol. 13, 696–698, September 1965.